

# Spinoptical metamaterials: spin-controlled photonics based on symmetry violation

Nir Shitrit, Igor Yulevich, Elhanan Maguid, Dror Ozeri, Dekel Veksler, Vladimir Kleiner, Erez Hasman\*

Micro and Nanooptics Laboratory, Faculty of Mechanical Engineering, and Russell Berrie Nanotechnology Institute, Technion – Israel Institute of Technology, Haifa 32000, Israel

\*mehasman@technion.ac.il

## ABSTRACT

Spinoptics provides a route to control light, whereby the photon helicity (spin angular momentum) degeneracy is removed due to a geometric gradient onto a metasurface. The alliance of spinoptics and metamaterials offers the dispersion engineering of a structured matter in a polarization helicity dependent manner. We show that polarization-controlled optical modes of metamaterials arise where the spatial inversion symmetry is violated. The emerged spin-split dispersion of spontaneous emission originates from the spin-orbit interaction of light, generating a selection rule based on symmetry restrictions in a spinoptical metamaterial. The inversion asymmetric metasurface is obtained via anisotropic optical antenna patterns. This type of metamaterial provides a route for spin-controlled nanophotonic applications based on the design of the metasurface symmetry properties.

**Keywords:** Spinoptics, metamaterials, metasurfaces, optical Rashba effect, inversion asymmetry, geometric phase, spin-orbit interaction, polarization, surface waves

## 1. INTRODUCTION

Metamaterials are artificial matter structured on a size scale generally smaller than the wavelength of external stimuli that enables a custom-tailored electromagnetic response of the medium. A new twist in this field originates from dispersion-engineered metamaterials. A peculiar route to modify the dispersion relation of an anisotropic inhomogeneous metamaterial is the spin-orbit interaction (SOI) of light; that is, a coupling of the intrinsic angular momentum (photon spin) and the extrinsic momentum<sup>1-3</sup>. Consequently, the optical spin provides an additional degree of freedom in nanooptics for spin degeneracy removal phenomena such as the spin Hall effect of light<sup>2,4-8</sup>. The chiral behavior originates from a geometric gradient associated with a closed loop traverse upon the Poincaré sphere generating the geometric Pancharatnam-Berry phase<sup>9,10</sup>. Specifically, spinoptics enables the design of a metamaterial with spin-controlled modes as in the Rashba effect in solids<sup>11-13</sup>.

The Rashba effect is a manifestation of the SOI under broken inversion symmetry (i.e., the inversion transformation  $\mathbf{r} \rightarrow -\mathbf{r}$  does not preserve the structure), where the electron spin-degenerate parabolic bands split into dispersions with oppositely spin-polarized states. This effect can be illustrated via a relativistic electron in an asymmetric quantum well experiencing an effective magnetic field in its rest frame, induced by a perpendicular potential gradient  $\nabla V$ , as represented by the spin-polarized momentum offset  $\Delta k \propto \pm \nabla V$ <sup>11-13</sup>. In terms of symmetries, the spin degeneracy associated with the spatial inversion symmetry is lifted due to a symmetry-breaking electric field normal to the heterointerface. Similar to the role of a potential gradient in the electronic Rashba effect, the space-variant orientation angle  $\phi(x, y)$  of optical nanoantennas induces a spin-split dispersion of  $\Delta k = \sigma \nabla \phi$ <sup>14,15</sup>, where  $\sigma_{\pm} = \pm 1$  is the photon spin corresponding to right and left circularly polarized light, respectively.

## 2. SPINOPTICAL METAMATERIAL ROUTE TO SPIN-CONTROLLED PHOTONICS

Here, we report on a spinoptical metamaterial that gives rise to a spin-controlled dispersion due to the optical Rashba effect (ORE). The inversion asymmetry is obtained in artificial kagome structures with anisotropic achiral antenna configurations (Figs. 1(a) and 1(b)) modeling the uniform ( $q = 0$ ) and staggered ( $\sqrt{3} \times \sqrt{3}$ ) chirality spin-folding modes

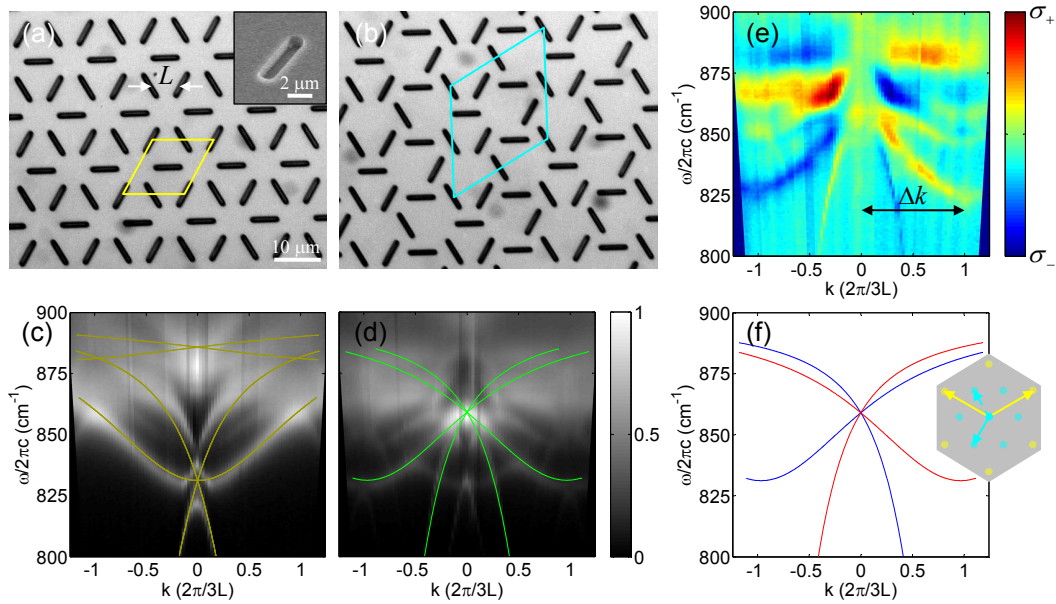


Figure 1. IS and IaS metamaterials and the ORE. (a), (b) Optical microscope images of  $q=0$  and  $\sqrt{3}\times\sqrt{3}$  structures, respectively. Rhombuses represent the corresponding unit cells in the real space. The inset in (a) is a scanning electron microscope image of the  $1\times 6\ \mu\text{m}^2$  antenna, etched to a depth of  $1\ \mu\text{m}$  on a SiC substrate. (c), (b) Measured intensity dispersions of thermal emission from  $q=0$  and  $\sqrt{3}\times\sqrt{3}$  structures at  $\varphi=60^\circ$ , respectively. Yellow lines in (c) correspond to the standard momentum-matching calculation; green lines in (d) highlight the new modes. (e), (f) Measured and calculated spin-polarized dispersions of the  $\sqrt{3}\times\sqrt{3}$  structure along the IaS direction of  $\varphi=60^\circ$ , respectively. The inset in (f) shows the reciprocal space of  $q=0$  (yellow) and  $\sqrt{3}\times\sqrt{3}$  (blue) structures with the corresponding reciprocal vectors; the dashed blue arrow indicates that only one of the  $\sqrt{3}\times\sqrt{3}$  reciprocal vectors is required to set the dispersion of a spinoptical metamaterial, in addition to both the  $q=0$  reciprocal vectors.

in the kagome antiferromagnet<sup>16</sup>. In the geometrically frustrated kagome lattice (KL), the reorder of the local magnetic moments transforms the lattice from an inversion symmetric (IS) to an inversion asymmetric (IaS) structure. Hence, the KL was selected as a platform for investigating the symmetry influence on spin-based manipulation of metamaterial dispersion.

We used the polarization anisotropy of a thermal antenna<sup>15</sup> in artificial kagome structures, where the anisotropic antennas are geometrically arranged in such a way that their principal axes are aligned with the original spin direction in the magnetic KL phases. These metamaterials with the nearest-antenna distance of  $L=6.5\ \mu\text{m}$  were realized using standard photolithographic techniques on a SiC substrate supporting resonant collective lattice vibrations (surface phonon polaritons (SPhPs)) in the infrared region. We measured angle-resolved thermal emission spectra at varying polar and fixed azimuthal angles ( $\theta, \varphi$ ), respectively, while heating the samples. The dispersion relation  $\omega(k)$  at  $\varphi=60^\circ$  of the  $q=0$  structure (Fig. 1(c)) exhibits good agreement with the standard momentum-matching calculation<sup>17</sup>. However, the measured dispersion of the  $\sqrt{3}\times\sqrt{3}$  configuration (Fig. 1(d)) reveals new modes as a result of the inversion asymmetry of the structure which may give rise to an optical spin degeneracy removal. By measuring the  $S_3$  component of the Stokes vector representing the circular polarization portion within the emitted light, we observed the  $\sqrt{3}\times\sqrt{3}$  spin-projected dispersion and found that the new modes yield a highly polarized emission with opposite spin states and a Rashba splitting of  $\Delta k = 2\pi/3L$  (Fig. 1(e)).

The removal of the spin degeneracy requires a spin-dependent correction to fulfill the momentum-matching equation. The spin-controlled dispersion of an IaS metamaterial obeys the spin-orbit momentum-matching (SOMM)

condition  $\mathbf{k}_e^{\parallel}(\sigma) = \mathbf{k}_{\text{SPP}} + m\mathbf{G}_1 + n\mathbf{G}_2 - \sigma\mathbf{K}_i$ , associated with two differentiated sets of reciprocal vectors: structural and orientational. Here,  $(\mathbf{G}_1, \mathbf{G}_2) = (\pi/L)(\mathbf{x} + \mathbf{y}/\sqrt{3}, -\mathbf{x} + \mathbf{y}/\sqrt{3})$  are the structural reciprocal vectors determined by the  $q = 0$  unit cell, whereas  $\mathbf{K}_{1,2} = (\pi/3L)(-\mathbf{x} \mp \sqrt{3}\mathbf{y})$  are the orientational reciprocal vectors determined by a  $\sqrt{3} \times \sqrt{3}$  unit cell (see Fig. 1(f) inset), associated with the local field distribution;  $\mathbf{k}_e^{\parallel}$  is the wavevector of the emitted light in the surface plane,  $\mathbf{k}_{\text{SPhP}}$  is the SPhP wavevector,  $(m, n)$  are the indices of the radiative modes, and  $i \in \{1, 2\}$  is the index of the specific spin-dependent geometric Rashba term. The SOMM condition arises from the combined contributions of the structural and orientational lattices resembling the structural and magnetic unit cells in the kagome antiferromagnet. We calculated the spin-dependent dispersion (Fig. 1(f)), confirming the  $S_3$  measured dispersion (Fig. 1(e)), with the optical Rashba spin-split.

The above condition can be also derived from symmetry restrictions, where the representation theory is applied to generate selection rules. When this procedure is implemented for the  $\sqrt{3} \times \sqrt{3}$  KL, which is invariant under a translation of  $2L$  to the left followed by a rotation of  $120^\circ$  counterclockwise, the SOMM condition is realized<sup>18</sup>.

In addition to the spin-projected dispersions, selection rules can also specify the direction of the surface wave excited at a given frequency. Hence, this concept serves as a platform for spin-controlled surface waves possessing excellent potential for manipulation on the nanoscale based on a geometric gradient.

The observed optical Rashba spin-split dispersions reveal two obvious relations of (i)  $\omega(k, \sigma_+) \neq \omega(k, \sigma_-)$ , which is a signature of inversion symmetry violation, and (ii)  $\omega(k, \sigma_+) = \omega(-k, \sigma_-)$ , which is a manifestation of time reversal symmetry (Figs. 1(e) and 1(f)). By measuring the  $S_3$  dispersion of the  $\sqrt{3} \times \sqrt{3}$  structure at varying  $\varphi$  and fixed  $\theta$ , we obtained the strength of the ORE pointing on the IS and IaS directions in the KL, where the IS directions of  $\varphi \in \{30^\circ, 90^\circ, 150^\circ\}$  are manifested by the spin degeneracy, while in all other directions the degeneracy is removed. Moreover, the symmetry-based approach offers an extended condition because it also recognizes the IS directions resulting in spin-degenerated dispersions with revealed new modes<sup>18</sup>.

The spin degeneracy removal was also shown in the near-field associated with the orbital angular momentum variation along the IaS directions. We revealed a chain of vortices with alternating helicities in the artificial  $\sqrt{3} \times \sqrt{3}$  building blocks, carrying a spin-dependent space-variant orbital angular momentum arising from the spiral phase front of the SPhPs<sup>18</sup>. The reported spin-based phenomena in the near- and far-fields inspire the development of a unified theory to establish a link between the spin-controlled radiative modes and the metasurface symmetry properties to encompass a broader class of metastructures from periodic to quasi-periodic or aperiodic. The design of metamaterial symmetries via geometric gradients provides a route for integrated nanoscale spintronic spinoptical devices based on spin-controlled manipulation of spontaneous emission, absorption, scattering, and surface-wave excitation.

### 3. SPIN-CONTROLLED PLASMONICS VIA OPTICAL RASHBA EFFECT

Surface plasmon polaritons (SPPs) are propagating surface-confined waves arising from the coupling of an electromagnetic field with collective oscillations of quasi-free electrons at the metal surface<sup>19</sup>. Plasmonic devices can confine light in regions with dimensions that are smaller than the wavelength of photons in free space<sup>20</sup>; hence, plasmonic metasurfaces have recently generated a considerable interest owing to their technological impact as the link between conventional optics and integrated on-chip photonics<sup>18,21,22</sup>. In this context, light manipulation on the nanoscale via electromagnetic surface waves provides the route for state-of-the-art miniaturized devices ushering in photonic nanocircuits. The resonant coupling of light to SPPs via metastructures is governed by the standard momentum-matching condition; so, once the structural properties are set, the excitation can be tuned by changing the light wavelength or angle of incidence<sup>23</sup>. Yet, the Rashba-induced geometric momentum correction can be either added to or subtracted from the light momentum owing to its spin-dependent origin; hence, light-matter interactions governed by momentum selection rules, such as the light coupling to plasmonic metastructures, are perturbed. In view of the ORE offers the engineering of light-matter interactions in a spin-based manner via the lattice symmetry breaking<sup>18</sup>, its alliance with plasmonics holds the promise for controlling SPPs by switching the light intrinsic spin.

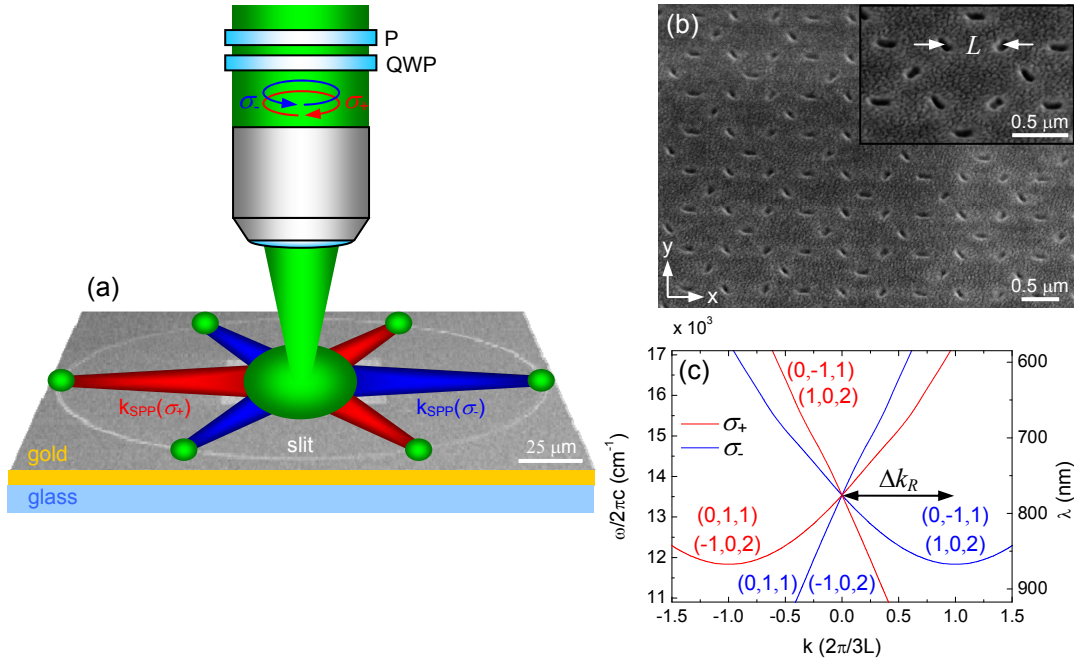


Figure 2. Spin-controlled plasmonics via the ORE. (a) Schematic setup for spin-based excitation of multidirectional SPP jets arising from the metasurface symmetry breaking. The antenna metastructure is normally illuminated with a laser light whose polarization is set by a circular polarizer (a linear polarizer (P) followed by a quarter-wave plate (QWP)) and propagating SPPs are free-space imaged with a decoupling slit. (b) Scanning electron microscopy image of the plasmonic  $\sqrt{3} \times \sqrt{3}$  KL metasurface consisting of  $80 \times 220$  nm<sup>2</sup> rectangular void antennas, etched to a depth of 60 nm upon 200 nm thick gold film; the 60  $\mu$ m square array was surrounded by a circular slit with a diameter of 180  $\mu$ m and a width of 100 nm. The inset shows the magnified region of the unit cell. (c) Calculated spin-projected dispersion of the  $\sqrt{3} \times \sqrt{3}$  configuration at the IaS  $x$  direction, via the SOMM condition. Red and blue lines correspond to  $\sigma_{\pm}$  incident spin states, respectively. Modes are specified with indices  $(m, n, i)$ .

We report on the experimental observation of the ORE in nanoscale plasmonics manifested by spin-controlled multidirectional excitation of SPPs under a normal-incidence illumination (see Fig. 2(a)). As a spin-controlled plasmonic metasurface for observing the ORE, we considered the anisotropic nanoantenna configuration of the artificial  $\sqrt{3} \times \sqrt{3}$  kagome structure (Fig. 2(b))<sup>18</sup>. The spin-projected dispersion relation of such an IaS metamaterial obeys the SOMM condition<sup>18</sup>. Accordingly, SPP jet is excited resonantly when the equation  $\mathbf{k}_{\text{in}}^{\parallel}(\sigma) = \mathbf{k}_{\text{SPP}} + m\mathbf{G}_1 + n\mathbf{G}_2 - \sigma\mathbf{K}_i$  is fulfilled; here,  $\mathbf{k}_{\text{in}}^{\parallel}$  is the wavevector of the incident light in the surface plane and  $\mathbf{k}_{\text{SPP}}$  is the SPP wavevector. Since we excite different modes in the optical Rashba spin-split dispersion (Fig. 2(c)), the directed plasmonic jets depend on both the wavelength and the polarization helicity of the incident light so for a given wavelength the excitation is spin-controlled.

In view of this, we fabricated by a focused ion beam the  $\sqrt{3} \times \sqrt{3}$  plasmonic metasurface consisting of rectangular void nanoantennas with  $L = 480$  nm, etched upon a thick gold film, evaporated onto a glass substrate (Fig. 2(b)). The square array was surrounded by a circular slit, where only the antenna metasurface was normally illuminated with a continuous wave Ti:sapphire tunable laser via a circular polarizer (see Fig. 2(a) for the experimental setup). The resonant illuminating wavelength of 740 nm was set according to the calculated spin-projected dispersion in the IaS direction of  $x$  axis (Fig. 2(c)), and the directional distribution of SPPs excited by the metasurface and decoupled by the slit were free-space imaged. In accordance with the 6-fold rotational symmetry of the  $\sqrt{3} \times \sqrt{3}$  KL and the vector summation representation of the SOMM condition (Figs. 3(c) and 3(d)), 3 plasmonic jets propagating to the 60°, 180° and 300° directions were measured for  $\sigma_{+}$  illumination (Fig. 3(a)); by flipping the spin to  $\sigma_{-}$  excitation, a mirror image is

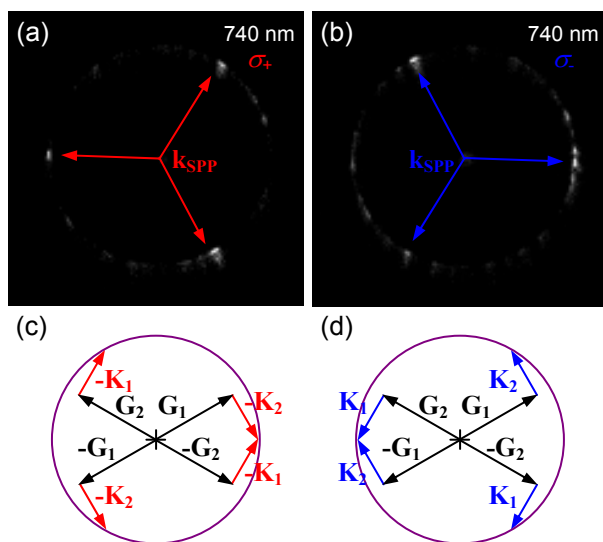


Figure 3. Experimental observation of the ORE in the plasmonic KL metasurface. (a), (b) Measured intensities of multidirectional SPP jets excited by the KL for  $\sigma_{\pm}$  illuminations, respectively, at a wavelength of 740 nm. (c), (d) Vector summation representation of the SOMM condition for  $\sigma_{\pm}$ , respectively. Note that  $\mathbf{k}_{\text{SPP}}$  is the complementary vector for the origin in the  $\mathbf{k}_{\text{SPP}}$  circle.

observed (Fig. 3(b)). Such a spin-controlled plasmonic metasurface holds the promise for spin-switch multidirectional guiding for surface-integrated multiport nanodevices based on the ORE. The reported phenomenon inspires the establishment of a link between a metasurface symmetry breaking and new selection rules with new degrees of freedom to encompass a broader class of light-matter interaction controls, ushering in a new era of light manipulation.

## REFERENCES

- [1] Liberman, V. S. and Zel'dovich, B. Y., "Spin-orbit interaction of a photon in an inhomogeneous medium," *Phys. Rev. A* 46, 5199-5207 (1992).
- [2] Bliokh, K. Y., Gorodetski, Y., Kleiner, V. and Hasman, E., "Coriolis effect in optics: unified geometric phase and spin-Hall effect," *Phys. Rev. Lett.* 101, 030404 (2008).
- [3] Litchinitser, N. M., "Structured light meets structured matter," *Science* 337, 1054-1055 (2012).
- [4] Hosten, O. and Kwiat, P., "Observation of the spin Hall effect of light via weak measurements," *Science* 319, 787-790 (2008).
- [5] Gorodetski, Y., Niv, A., Kleiner, V. and Hasman, E., "Observation of the spin-based plasmonic effect in nanoscale structures," *Phys. Rev. Lett.* 101, 043903 (2008).
- [6] Bliokh, K. Y., Niv, A., Kleiner, V. and Hasman, E., "Geometrodynamics of spinning light," *Nature Photon.* 2, 748-753 (2008).
- [7] Shitrit, N., Bretner, I., Gorodetski, Y., Kleiner, V. and Hasman, E., "Optical spin Hall effects in plasmonic chains," *Nano Lett.* 11, 2038-2042 (2011).
- [8] Yin, X., Ye, Z., Rho, J., Wang, Y. and Zhang, X., "Photonic spin Hall effect at metasurfaces," *Science* 339, 1405-1407 (2013).
- [9] Berry, M. V., "The adiabatic phase and Pancharatnam's phase for polarized light," *J. Mod. Opt.* 34, 1401-1407 (1987).
- [10] Bomzon, Z., Kleiner, V. and Hasman, E., "Pancharatnam-Berry phase in space-variant polarization-state manipulations with subwavelength gratings," *Opt. Lett.* 26, 1424-1426 (2001).
- [11] Dresselhaus, G., "Spin-orbit coupling effects in zinc blende structures," *Phys. Rev.* 100, 580-586 (1955).
- [12] Rashba, E. I., "Properties of semiconductors with an extremum loop. 1. Cyclotron and combinational resonance in a magnetic field perpendicular to the plane of the loop," *Sov. Phys. Solid State* 2, 1109-1122 (1960).

- [13] Ishizaka, K., Bahramy, M. S., Murakawa, H., Sakano, M., Shimojima, T., Sonobe, T., Koizumi, K., Shin, S., Miyahara, H., Kimura, A., Miyamoto, K., Okuda, T., Namatame, H., Taniguchi, M., Arita, R., Nagaosa, N., Kobayashi, K., Murakami, Y., Kumai, R., Kaneko, Y., Onose, Y. and Tokura, Y., "Giant Rashba-type spin splitting in bulk BiTeI," *Nature Mater.* 10, 521-526 (2011).
- [14] Dahan, N., Gorodetski, Y., Frischwasser, K., Kleiner, V. and Hasman, E., "Geometric Doppler effect: spin-split dispersion of thermal radiation," *Phys. Rev. Lett.* 105, 136402 (2010).
- [15] Frischwasser, K., Yulevich, I., Kleiner, V. and Hasman, E., "Rashba-like spin degeneracy breaking in coupled thermal antenna lattices," *Opt. Express* 19, 23475-23482 (2011).
- [16] Grohol, D., Matan, K., Cho, J.-H., Lee, S.-H., Lynn, J. W., Nocera, D. G. and Lee, Y. S., "Spin chirality on a two-dimensional frustrated lattice," *Nature Mater.* 4, 323-328 (2005).
- [17] Ebbesen, T. W., Lezec, H. J., Ghaemi, H. F., Thio, T. and Wolff, P. A., "Extraordinary optical transmission through sub-wavelength hole arrays," *Nature* 391, 667-669 (1998).
- [18] Shitrit, N., Yulevich, I., Maguid, E., Ozeri, D., Veksler, D., Kleiner, V. and Hasman, E., "Spin-optical metamaterial route to spin-controlled photonics," *Science* 340, 724-726 (2013).
- [19] Brongersma, M. L. and Shalaev, V. M., "The case for plasmonics," *Science* 328, 440-441 (2010).
- [20] Schuller, J. A., Barnard, E. S., Cai, W., Jun, Y. C., White, J. S. and Brongersma, M. L., "Plasmonics for extreme light concentration and manipulation," *Nature Mater.* 9, 193-204 (2010).
- [21] Kildishev, A. V., Boltasseva, A. and Shalaev, V. M., "Planar photonics with metasurfaces," *Science* 339, 1232009 (2013).
- [22] Zheludev, N. I. and Kivshar, Y. S., "From metamaterials to metadevices," *Nature Mater.* 11, 917-924 (2012).
- [23] Drezet, A., Koller, D., Hohenau, A., Leitner, A., Aussenegg, F. R. and Krenn, J. R., "Plasmonic crystal demultiplexer and multiports," *Nano Lett.* 7, 1697-1700 (2007).